Journal of Imaging Science and Technology® 53(4): 041208–041208-8, 2009.

Links Between Ink Rheology, Drop-on-Demand Jet Formation, and Printability

S. D. Hoath▲, I. M. Hutchings and G. D. Martin▲
Department of Engineering, Institute for Manufacturing, University of Cambridge, Mill Lane, Cambridge CB2 1RX, United Kingdom
E-mail: sdh35@cam.ac.uk

T. R. Tuladhar, M. R. Mackley and D. Vadillo
Department of Chemical Engineering, University of Cambridge, Pembroke Street, Cambridge CB2 3RA, United Kingdom

Abstract. *This article links measurements of ink jetting performance in drop-on-demand printing with the high-frequency rheological properties of model viscoelastic fluids containing linear polymers with various molecular weights. Jet formation and evolution were studied for solutions of polystyrene in diethyl phthalate. Ligament length, initial jet ejection speeds, and ligament extension and retraction rates were determined by high-resolution imaging with high time resolution. For these fluids, the viscosity measured under low shear-rate conditions showed no correlation with their jetting performance. The jetting behavior was, however, well correlated with high frequency rheological properties measured at 5 kHz using a piezoelectric axial vibrator rheometer. This study shows that high frequency rheometry can provide useful predictive data about the jettability of fluids, and differentiate between inks that have similar low shear-rate viscosity yet show different jetting behavior. A phenomenological model has been proposed and fitted to the evolution of the average ligament length from emergence, through break-up and into the final state of unmerged drops and associated satellites in order to help discuss the influence of viscoelastic behavior on the fixed speed drop-on-demand jetting and printability of fluids. The values of the parameters of this model obtained from the fitting are shown to have a consistent correlation with the rheological properties of the jetted fluids. © 2009 Society for Imaging Science and Technology.*
[DOI: 10.2352/J.ImagingSci.Technol.2009.53.4.041208]

INTRODUCTION

Previous research[1–5] has shown that useful information about ink jet fluid behavior can be extracted from the detailed optical study of drop-on-demand ink jets and ligaments. The level of excitation actuation required to achieve a certain speed (say, 6 m/s) at a typical printing distance of ~1 mm from the nozzle can be used to characterize an important property of the fluid. Fluids with low values of low shear-rate viscosity require low actuation levels and the ligament extends almost linearly with time until it detaches; higher viscosity fluids need stronger actuation, and the jet decelerates more rapidly after emergence and detaches later. It is well known that viscoelasticity can affect ligament breakup,[6] so when an ink jet fluid exhibits viscoelastic behavior the value of its low shear-rate viscosity may not fully reflect the resistance to flow through the nozzle or the deceleration of the ligament. This is one reason why the characterization of real inks for drop-on-demand printing is particularly challenging.

Ink jet fluids are usually characterized by their zero shear rate viscosity and sometimes the apparent viscosity is measured as a function of shear rate to establish any shear thinning behavior. Measurements[7] indicate that most ink jet fluids do not show significant thinning even at high shear rates. Because the viscoelastic effects within ink jet fluids occur with very short time scales, it is not possible to measure effects due to linear viscoelasticity using most mechanical oscillation rheometers. Recently however a piezoaxial vibrating (PAV) rheometer has been developed at the University of Ulm[8] that does enable high frequency viscoelastic properties to be readily measured for low viscosity fluids that contain small, but important viscoelastic components.

The rheological behavior of viscoelastic fluids is commonly represented in terms of complex viscosity $\eta^*(=\eta' - i\eta'') = G^*/i\omega$, where $G^*(=G' + iG'')$ is the complex modulus at angular frequency ω $(=2\pi f$ at frequency $f)$. G' represents the elastic (storage) component and G'' the viscous (loss) component. The magnitude of G^* is determined by $|G^*|^2 = G'^2 + G''^2$. At low frequency, the viscous modulus $G'' \approx \eta_0\omega$ while the elastic modulus $G' \approx 0$; laboratory measurements of viscosity are typically carried out at such low frequencies (<100 Hz) that they determine only G''. However, the time scales involved in the generation of jets and drops in drop-on-demand printing correspond to frequencies some 100 times greater[9] and for viscoelastic fluids the elastic effects may become highly significant. The PAV rheometer is able to explore viscoelastic properties in the frequency range from 1 to 10,000 Hz.

Filament-stretching rheometry of polymer solutions can be also used to explore their extensional rheology.[7] In particular, the way in which a filament stretches[9] can be used to identify nonlinear viscoelasticity effects that the PAV is not

▲IS&T Member.

Received Dec. 11, 2008; accepted for publication Mar. 2, 2009; published online Jun. 2, 2009.
1062-3701/2009/53(4)/041208/8/$20.00.

able to detect. Thus a combination of PAV linear viscoelastic data and filament stretching nonlinear data can be compared with ink jet performance.

The presence of polymer, pigment particle additives, dispersant, binder, and other components can all affect the base viscosity and viscoelastic properties of an ink jet fluid. The present work examines the correlation between jet production from a commercial ink jet head, described in terms of ligament length, initial jet ejection speeds and ligament extension and retraction rates, and rheological measurements made on the same fluids at 5 kHz with a PAV rheometer for a range of model viscoelastic fluids containing polystyrene as a solute.

Setting up ink jet systems for desired performance levels, such as drop speed at the substrate location and the average length of the ligament at break off, often relies upon real-time imaging systems based on stroboscopic light sources, such as light-emitting diode or xenon flash lamps, viewed by eye as either the drive pulse voltage, the timing between the ejection drive pulse and the flash, or both are varied. As is well known, while providing a practical means of assessing conditions this procedure does tend to smear out those parts of the ink jet tail that are intrinsically variable due to the nature of the break-up process or are rapidly time varying. High speed spark flash images can be used to obtain quantitative timed information such as satellite size and spacing distributions;[3] in this article we concentrate on the evolution over time of the average ligament length determined from such images using a phenomenological model to help understand the links between the ink rheology, drop-on-demand jet formation, and the influence of jetting on overall printability.

EXPERIMENTAL METHODS AND MATERIALS

Model Fluids

Model fluids were prepared with an effectively constant value of low shear-rate viscosity ($\eta_0 = 19 \pm 2$ mPa s at 21 ± 1°C) by dissolving monodisperse polystyrene (PS) in diethyl phthalate (DEP) (with a viscosity of 10 mPa s). Four different molecular weights of PS were used: 24 kDa (designated PS24), 75 kDa (PS75), 110 kDa (PS110), and 210 kDa (PS210). Two series of solutions were prepared: using PS110 (from 0 to 1 wt %) with enough PS24 added ($\leq$2.5 wt %) to achieve the target viscosity, and using PS210 (from 0 to 0.6 wt %) with added PS75 ($\leq$1.0 wt %).

Rheometry

The principles of PAV squeeze flow rheometry have been fully described elsewhere.[8] In this method a thin film of the liquid is trapped between two plates, and its response to high frequency oscillatory compression is determined. The technique perturbs a 10–100-μm-thick fluid sample with a fixed and small ($\sim$10 nm) amplitude wave and detects in-phase and out-of-phase responses; the high frequency limit of $<$10 kHz for the present PAV equipment design is set by operating below the resonance frequency of the PAV. In addition, the successful application of PAV in the present work required that the fluid samples did not contain trapped bubbles since these could significantly contribute toward sample compressibility and could even dominate the elastic effects of the viscoelastic fluid; similarly, large bubbles have been found to disrupt the normal fluid ejection mechanisms in ink jet print heads.[10]

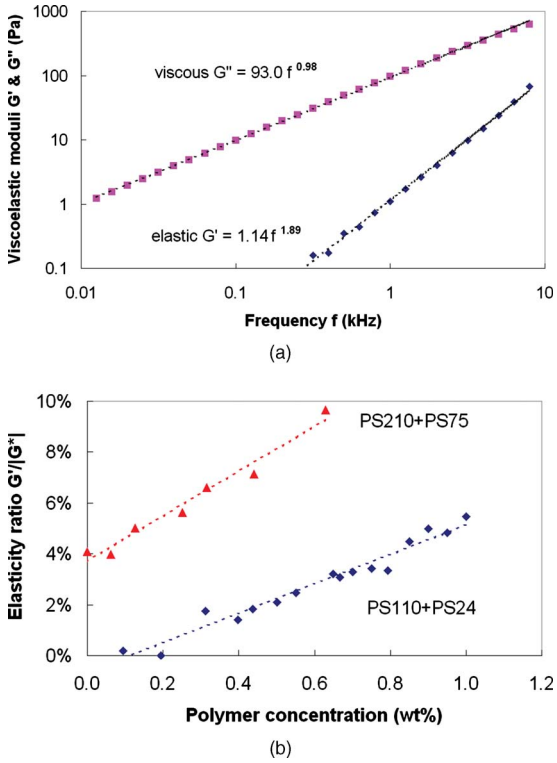

Figure 1. (a) Viscoelastic moduli G' and G'' (Pa) determined by PAV as a function of frequency f (kHz) for the 1 wt % PS110 solution. (b) Elasticity ratio $G'/|G^*|$ measured at 5 kHz for both fluid series, as indicated. All fluids had essentially the same low shear-rate viscosity but the content of the higher molecular weight polymer (shown on the x axis) was varied.

The method allows the viscoelastic moduli G' and G'' to be determined in a short time over a frequency range of $\sim$3 decades. Figure 1(a) shows the typical variation of G' and G'' with frequency for one of the fluid samples, as measured by the PAV method. The ratio $G'/|G^*|$ evaluated at 5 kHz (a frequency chosen below the maximum frequency limit, giving consistent elasticity results, and close to the 4 kHz value used by other PAV workers[8]) was used as a measure of the degree of elasticity to characterize the model fluids in the present work. The elasticity ratio $G'/|G^*|$ for the fluid containing 1 wt % PS110 in DEP was $\sim$6% at 5 kHz; as discussed below this particular fluid has sufficient elasticity to disrupt its jetting, although at this frequency the effect of G' on the value of $|G^*|$ is still very small. Such weak elasticity would not be detectable by low frequency measurements made using any conventional low shear viscometers.

Jetting and Data Analysis

The model fluids were jetted at room temperature with a Xaar XJ126-200 drop-on-demand print head using the same pull-push waveform timings throughout but adjusting the piezodrive level for each fluid to achieve a drop speed of

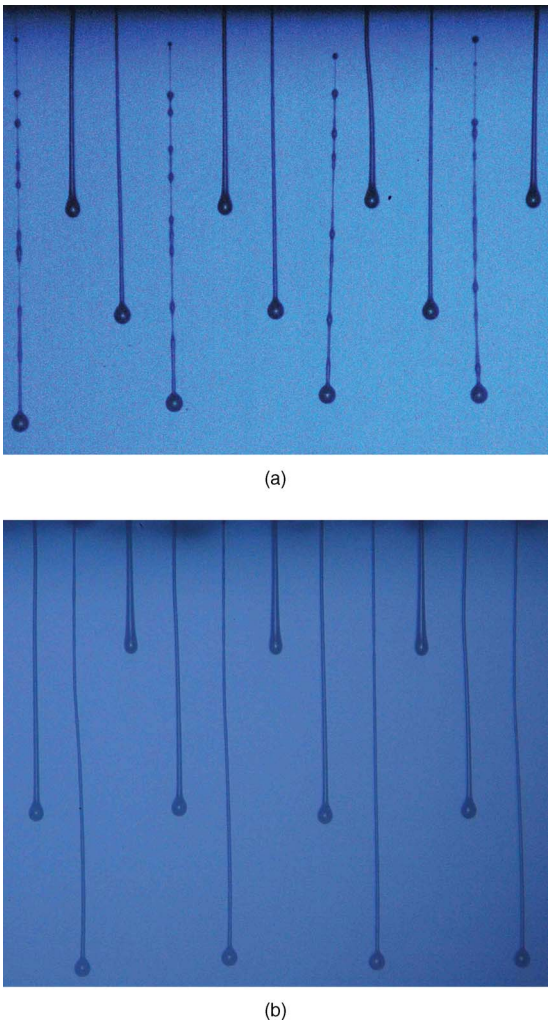

Figure 2. High speed flash images (field of view in each case 1.2×1.4 mm^2) showing jets formed with model fluids (a) near the limit for jetting (0.25% PS210+PS75+DEP) and (b) above the limit for jetting (0.4% PS210+PS75+DEP).

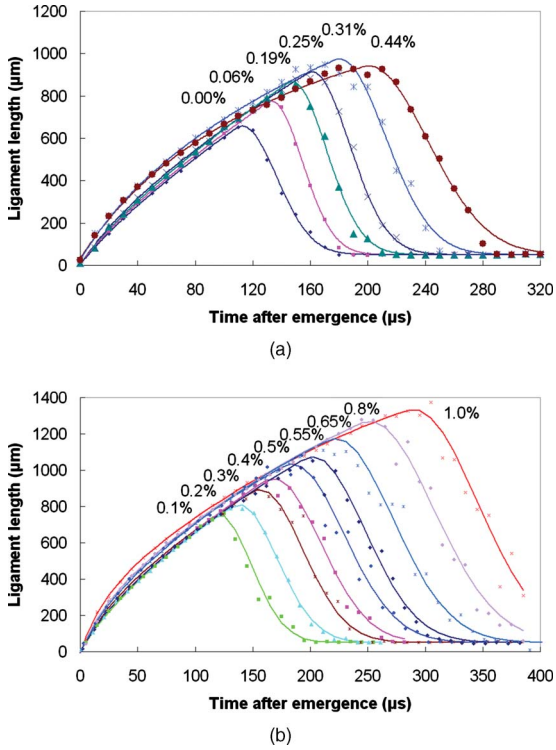

Figure 3. Ligament length of the main (leading) drop vs time after emergence for main drop speed ~6 m/s at 1 mm distance. Each curve in each graph is labeled with the concentration of the higher molecular weight polymer in the solution (wt %): (a) shows PS210+PS75 data and (b) shows PS110+PS24 data.

~6 m/s at 1 mm printing distance. The jets and drops were analyzed by high speed imaging, based on very rapid (~20 ns) single flash photography, as described earlier.[1–3]

Figure 2(a) shows an example of a typical image for fluid jets close to 1 mm length but still below the maximum polymer concentration limit for the generation of drops at ~6 m/s. The systematic timing difference between adjacent nozzles assists the visualization of the progression between jetting and the formation of beads on the long ligaments, which are <3 μm in diameter at the top in the cases where they have detached from the nozzles. These ligaments still connect all the ejected fluid. Images obtained with increased delays can track the final fate of the ligaments to determine whether they collapse to form a single drop or break-up into multiple satellites, or for higher polymer concentrations, whether the ligaments ever detach from the nozzle plane. Figure 2(b) shows an example of an image for a fluid with higher polymer concentration, above the maximum concentration which gives drops. Long ligaments that do not detach can subsequently retract fully back into the nozzle, while at yet higher polymer concentration the fluid may never emerge from the nozzle.

In the present work, several jets were included in each image to allow the average ligament behavior to be determined over a range of nozzles. This technique is in contrast to the study of jet formation from a single nozzle.[4,11,12] The need to extract quantitative data on jet dimensions from a wide field of view meant that corrections had to be applied for image distortions, the most significant of which was a variation in magnification by up to ~2% across the image. Print frequencies (drop ejection rates) of 1.5–3 kHz were also used for each fluid sample in order to provide a more realistic representation of printing conditions than simply studying the ejection of isolated jets.

RESULTS

Rheometry

Although the low shear-rate viscosities of the fluids lay within a narrow range ($\eta_0 = 17.5-20.7$ mPa s at ~21 °C), the ratio $G'/|G^*|$ at 5 kHz determined by the PAV method (at ~25 °C) rose almost linearly with the concentration of the higher molecular weight polymer for both series of model fluids, as shown above in Fig. 1(b). The variations in G' and G'' with frequency, for one of the fluid samples, are plotted in Fig. 1(a) and show power law behavior. The power law exponents of 1.89 for elastic modulus G' and 0.98 for viscous modulus G'' are close to the theoretical values of 2 and 1, respectively, as predicted theoretically for a simple

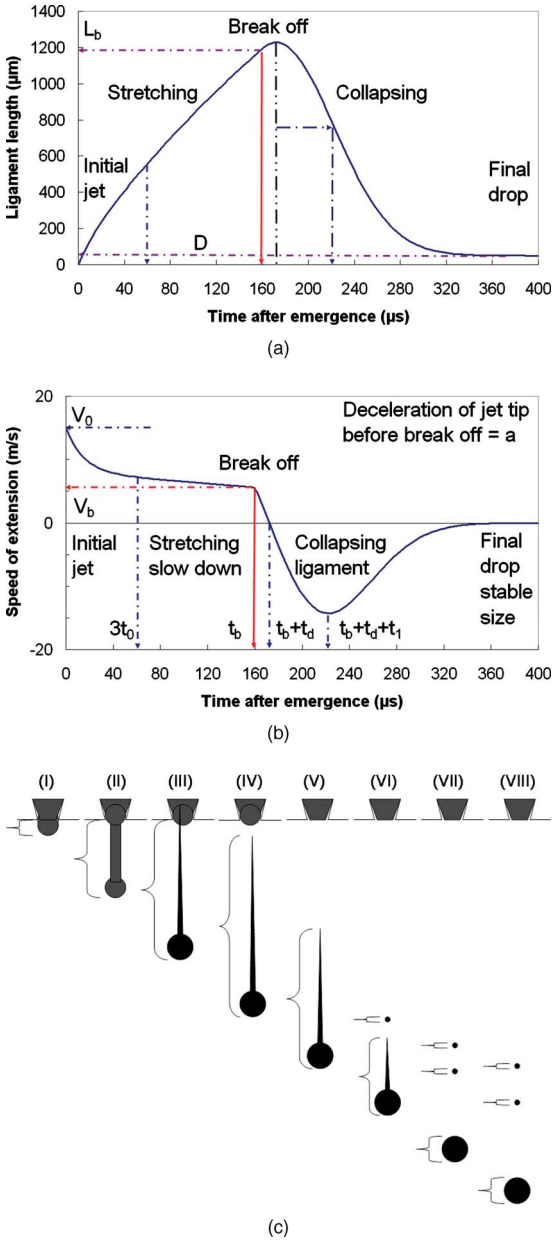

Figure 4. (a) Model for ligament length attached to the main drop showing evolution with time after emergence for the main drop speed V_1 ~6 m/s at 1 mm distance. The ligament length at break-up is L_b and the final main drop diameter is D; between these states the ligament length remaining attached to the main drop is represented by a Gaussian shape. (b) shows the extension speeds implicit in this representation; speed is continuous at break-off time t_b so that the ligament length can continue to stretch for a short time t_d after break off, and after attaining this maximum extension, the ligament recoil reaches a maximum speed after further time t_1. (c) is a schematic diagram for an ink jet depicting ligament length (shown by the braces in each case) at various times: (I) near emergence, (II) stretching, (III) break-up length L_b at time t_b, (IV) maximum length at delay time t_d later, (v) tail recoiling, (VI) satellite formation (if any), (VII) final length state D, and (VIII) downstream drift of final length state D.

Maxwell model linear viscoelastic fluid.[13] The value of $G'/|G^*|$ remained below 10% for all the fluids up to the highest (~10 kHz) PAV frequency. No elasticity was detected in the pure solvent (DEP) at 5 kHz (i.e., $G'/|G^*| \approx 0$). The expected variation in $G'/|G^*|$ with polymer content is discussed elsewhere.[7]

Jetting Behavior and Ligament Length

The total length of the main drop and attached ligament, measured from high speed images captured at different times after initial ejection, is plotted against time in Figure 3(a) for the fluids containing both PS210 and PS75. As the concentration of PS210 (the higher molecular weight component) was increased, more actuation was needed to achieve the target velocity of ~6 m/s at 1 mm, deceleration of the ligament before it detached became greater, and the detachment time increased, despite the near equality of the low shear rate viscosities across the series. There is a significant effect on jetting, which varies with polymer concentration, unexplained by the low shear rate viscosities of the fluids. The main drop diameter at long times was also found to be independent of the polymer concentration; but as the polymer concentration increased, the total volume of fluid ejected and the total ligament volume both increased. The satellites produced by subsequent breakup of the ligament did not merge into the main drop even well beyond 1 mm from the nozzle plane. Similar results are shown in Fig. 3(b) for the other fluid series (PS110+PS24): this could be jetted at somewhat higher concentrations than the first fluid series (PS210+PS75).

Figure 4(a) shows features of the analytic representation of ligament length (including attached drop) used in this work. The empirical ligament length curves shown in Fig. 3 are matched at the jet detachment time (break-off time t_b). Our model parameters for total ligament length before the break off are the emergent tip speed V_0, target speed V_1 for the main drop at 1 mm, the decay time t_0 for the initial stage decay of the emergent tip speed V_0 toward speed V_1, the deceleration of the tip just before break off a, and the break-off time t_b. The values of V_0 and t_0 are only significant for the ligament lengths at times well before the break-off time, while the assumed constant deceleration rate is mainly linked to the ligament behavior immediately before the break-off time. The length and speed of the ligament length extension are continuous at the break-off position and, as can be seen in Fig. 4(a), can lead to an elongated length just behind the break-off point. (Note that the tip speed V_b at break off does not usually have exactly the same value as the main drop target speed V_1 at 1 mm.)

Our earlier[1] data on pure DEP solvent jets at ~6 m/s showed that emergent Newtonian fluid lengths can be well represented by

$$L(t_b \geq t > 0) = V_1 t + \alpha(1 - \exp(-t/t_0)), \qquad (1)$$

where α is a constant. A simple constant deceleration term appears adequate for the purpose here of matching the polymeric fluid ligament lengths and speeds.

The lengths of the ligament at time t up to the break-off time t_b are given by

$$L(t_b \geq t > 0) = V_1 t + (V_0 - V_1)t_0(1 - \exp(-t/t_0)) - \frac{1}{2}at^2. \tag{2}$$

This form for the ligament length implies that the speeds of the tip, shown in Fig. 4(b), at times up to break off are given by

$$V(t_b \geq t > 0) = \frac{d}{dt}(L(t_b \geq t > 0)$$

$$= V_1 + (V_0 - V_1)\exp(-t/t_0) - at. \tag{3}$$

The emergent tip speed $V(t=0)=V_0$; the tip slows with constant deceleration a for times $t \gg 3t_0$, while for early times the tip deceleration decays exponentially with a characteristic timescale t_0 toward the target speed V_1 in the absence of the later deceleration. The final drop diameter D and the ligament collapse time scale t_1 are the extra parameters introduced to describe the ligament length after the break-off time. At long times, the ligament length collapses either to the average diameter D of the main drop [see Fig. 4(a)] or to a longer length including the average size of satellites. Our conclusions about the collapse time scale t_1 for the fluids studied are not significantly affected by whether D represents the total ink length or the main drop. The present work aims to represent the overall collapse time scale t_1 after the ligament break-off time without assuming that time scale t_1 links to ligament behavior prior to the break-off time.

The length of the ligament after break-off time t_b is given by

$$L(t > t_b) = D + (L_b - D)\exp\left(\frac{1}{2}(t - t_b)(t_b + 2t_d - t)/t_1^2\right), \tag{4}$$

where D is the final length of the ink drop, L_b is the break-off length, and t_1 is the time scale for the Gaussian collapse. This form of length clearly satisfies matching at $t=t_b$ and has a well determined asymptotic value D; it also has a maximum length occurring after the break off, centered on a time t_b+t_d, where

$$t_d = t_1^2 V_b/(L_b - D). \tag{5}$$

This delay time ensures that the ligament velocities are also matched either side of the break-off time for the choice of a Gaussian function to represent the collapsing ligament length. The implied ligament length extension is often smaller than D and unseen in practice. The prebreak- and postbreak-off accelerations are not matched in our assumptions: these should not be matched because the prebreak-off deceleration is that of the jet tip mass caused by the ligament still attached to the nozzle plane whereas the postbreak-off deceleration is caused by recoil of the low mass tail of the highly stretched thin ligament toward the tip mass. The maximum negative speed of the ligament extension after break off occurs at the time $t=t_b+t_d+t_1$, i.e., at the time t_1 after the peak in the ligament length has been attained, arising automatically from the properties of a Gaussian shape with characteristic time scale t_1.

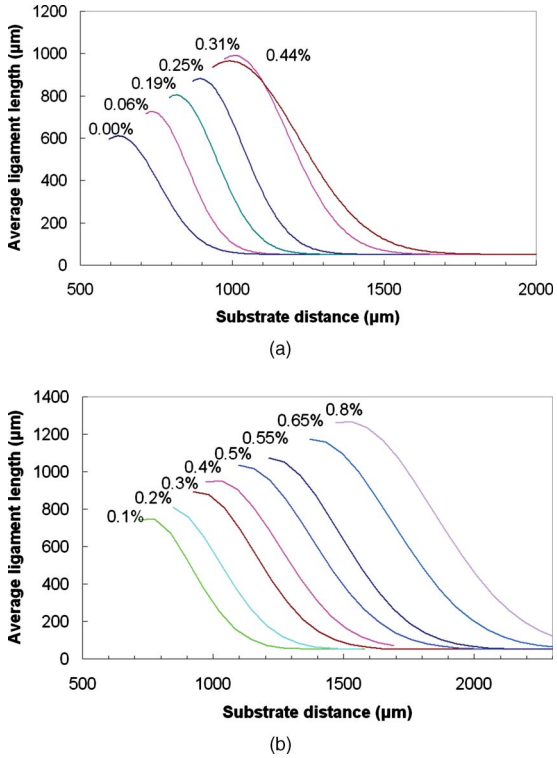

Figure 5. Instantaneous ligament length, after detachment from the nozzle, plotted against the distance traveled by the jet tip. Each curve is labeled with the concentration of the higher molecular weight polymer in the solution (wt %): (a) PS210+PS75 and (b) PS110+PS24.

Within this empirical representation, should the break-off time t_b be extended in proportion to t_1 by the polymer effects and the jet be fast enough that the break-off length increases approximately linearly with time t_b, then the delay time t_d between the break off and the attainment of maximum ligament length is more nearly proportional to the collapse time scale t_1 than to t_1^2. Since the ligament break-off length L_b greatly exceeds D for the polymer fluids tested, then Eq. (5) gives

$$t_d \approx t_1^2 V_b/L_b \approx t_1^2/t_b \propto t_1. \tag{6}$$

However, we will use our empirical model fits to establish the existence of such correlations, rather than assume them.

Figures 5(a) and 5(b) show the instantaneous total ligament length after the jet had detached from the nozzle plane as a function of the distance traveled by the tip of the jet, derived from the data plotted in Figs. 3(a) (for PS210+PS75) and Fig. 3(b) (for PS110+PS24), respectively. These curves are shown extending well beyond the normal substrate location of 1 mm, as derived from our analytical representation of ligament length shown as the continuous lines in Figs. 3(a) and 3(b).

Elasticity and Jet Detachment Time

Correlations were found between the elasticity ratio $G'/|G^*|$ for the fluid and the time at which the ligament detached

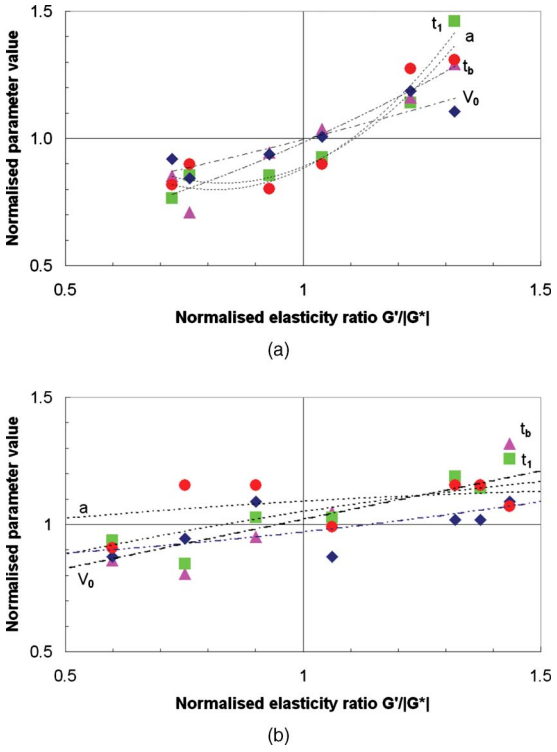

Figure 6. Model parameters for emergence speed V_0 (◆), deceleration a before break-off time (●), break-off time t_b (▲), and Gaussian time t_1 (■) as described in the text as a function of the elasticity ratio $G'/|G^*|$ using normalization by the average values in both axes found for (a) PS210+PS75 and (b) PS110+PS24.

from the nozzle (the break-off time t_b), the emerging speed V_0 with which the fluid left the nozzle to achieve a final speed of 6 m/s after 1 mm travel, the deceleration a of the jet tip before break off, and the characteristic time scale t_1 of the ligament recoil process. Figure 6 shows the normalized values for the jet emergence speed (◆), deceleration a before break-off time (●), break-off time t_b (▲), and Gaussian time scale t_1 (■) against the normalized elasticity ratio: each variable is normalized by their average value over the elasticity ratio span and show similar trends for both sets of fluids.

The break-off time t_b and the emerging jet speed V_0 increased roughly linearly with $G'/|G^*|$, suggesting that they are linked with the fluid elasticity; the ligament recoil time scale t_1 and the deceleration of the jet tip before break-off a show nonlinear relationships which differ for the two sets of fluids in ways that will be discussed in terms of polymer theory elsewhere.[13] Here we can link the empirically determined emerging jet speed V_0 and the subsequent break-off time t_b to the linear viscoelastic character of the jetted fluid.

Our lack of data for elasticity ratios below ~4% for PS210 fluids restricts the normalized elasticity ratio span in Fig. 6(a). This paucity of data arises from the fact that PS75 was added to PS210 fluids to achieve a constant viscosity: this polymer has significant elasticity, most evident as $G'/|G^*|$ ~4% for the samples with lowest concentration of PS210, which include several wt% of PS75. The use of lower concentrations of PS75 in the PS210+PS75 series would have resulted in significantly lower low shear viscosity than the nominal value of 19 mPa s and would have prevented direct comparisons of the jetting results for the PS210 and PS110 series at the same nominal low shear viscosity. A similar method of viscosity adjustment was used for the PS110 series, but the elasticity of the PS24 used was much lower even at its highest content and so the normalized elasticity ratio data for PS110 start at 0. In addition the normalized elasticity ratio span available for the PS110 parameters was nearly double that for the PS210 parameters, extending to ~2.4, so a more restricted span for normalized elasticity ratio is used in both Figs. 6(a) and 6(b) in order to highlight the differences between as well as the trends in common for these two polymer fluids. Trend lines shown dotted were fitted to the full range of data in all cases, not just to the region of the span.

DISCUSSION

The fluids used in this study were designed to have very similar values of viscosity measured at low shear rates but showed a wide range of elastic behavior as determined by the PAV method at 5 kHz and as shown in Fig. 1. The elasticity, expressed as the ratio of the moduli $G'/|G^*|$, was on the order of three times as high for the fluids containing the higher molecular weight polystyrene (210 kDa) as for the fluids containing the same concentration by weight of the lower molecular weight polymer (110 kDa). If expressed in terms of molecular concentration the difference in elasticity between the two sets of fluids was even more pronounced. These differences in elastic properties had a strong effect on the jetting behavior of the fluids in drop-on-demand printing. The fluids containing PS210 exhibited typical time scales and jet decelerations which were about two thirds of the values for those containing PS110 for similar values of elasticity ratio $G'/|G^*|$. This empirical result, suggesting that PS210 could be a better ink jet additive than PS110, is examined elsewhere.[13]

Our phenomenological model and the computed curves shown in Fig. 4 provide a fairly simple representation for the average ink jet behavior that we have measured for fluids which have low shear-rate viscosity values ~20 mPa s and jetting at ~6 m/s. The work by Dong et al.[4] concentrated on imaging various fluids with low shear-rate viscosities of 1–5 mPa s and break-off speeds of ~3–6 m/s. We find for fluid jetted at somewhat lower speed and low-shear viscosities, the ligament shape and break-up into main drops and multiple satellites is somewhat different from that we have shown in Fig. 2, although the same phenomenological model approach can be applied. The most significant difference seen in jetting lower viscosity fluids at 6 m/s is that the main drop breaks off at a similar time to the ligament tail break off and that the remaining ligament length collapse time is much longer; this sort of behavior confirms the trend of our phenomenological model to overpredict the average ligament lengths at elapsed times just prior to attainment of the final stable length. When the jetting speed is slower, fluid may detach at the ligament tail end but never break-up any

further, just forming a single final drop. Our phenomenological model has enabled an interpretation based on the observed ligament length to be used despite the formation of satellites: in fact it is not concerned with the formation of satellites but with the average disposition of the ink along the jetting axis.

Knowing from analysis of images the size of final main drop diameter and the typical unmerged satellite for the fluid jetted at that speed, we can represent the final length on average as a main drop and a (noninteger) number of such satellites that accompany it. When the speed of the jetting for an application has to be maintained irrespective of the fluid, minimizing the final length can be used to choose an appropriate fluid, while the time taken to reach this final length determines the substrate distance and the maximum print rate. Our model's characterization, by a one parameter Gaussian shape, of the average ligament length during the collapse after break off, gives this time; alternative approaches based on physically modeling the collapse of the ligament length for ink jets will be reported elsewhere.[13]

The curves in Fig. 5 show that while the final main drop size may be independent of the polymer concentration, the overall length of the ligament increased markedly with the elasticity of the fluid. In order to achieve the same jet tip or drop velocity at a nozzle-substrate distance of 1 mm, greater actuation was needed for the more elastic fluids, which resulted in the ejection of a greater total volume of fluid. In most applications, short ligament lengths at the break-off time are preferable, but where high speeds are required to maintain high drop ejection rates it is helpful to be able to predict how the fluid gets distributed on average at certain delay times and distances after ejection so that some sensitivity to the fluid constitution for particular applications can be assessed. Clearly the recoil speed and the average length are not the whole story, as they do not (and cannot readily) account for the transverse angular spread associated with the break-off regime.

Plots such as Fig. 5 can be used to help determine the maximum polymer concentration which is compatible with a specified average ligament length for a certain nozzle-substrate separation by determining the overall ligament length at the point where the jet tip would strike the substrate. A greater standoff distance may produce a more compact print region, as ink in the ligament and satellites has time to recombine with the main drop, at the expense of poorer drop placement caused by the break-up process, geometrical, and aerodynamic effects.

Our one-dimensional ligament length model clearly only represents a part of real ink jet applications, albeit we believe, an important part. Since the substrate is usually translating orthogonally to the drop direction the ligament, if it is sufficiently long when it reaches the substrate, may appear on the substrate as an elongation to the printed dot. This is objectionable because line edges are no longer smooth. On the other hand, when printing multiple drops at typical ejection rates (10–50 kHz), the head of the second drop may well merge with the tail of the preceding drop from a different nozzle. This may result in a line segment with smooth long sides, which is desirable. Therefore our model does not imply that, and we cannot claim, increasing the nozzle-substrate separation will inevitably improve printing quality, but an optimization, balancing a shorter ligament length against the detrimental effects of increasing separation may be appropriate.

A characteristic timescale associated with the ejection of a fluid jet can be estimated from the nozzle diameter divided by the fluid ejection speed; for the present conditions this is approximately $50\ \mu\text{m} \div 10\ \text{m/s} = 5\ \mu\text{s}$. The time scale for detachment of the ligament and its collapse is in contrast $\sim 100\ \mu\text{s}$ (see Fig. 3). It is thus clear that although rheological measurements at 5 kHz (corresponding to a timescale of $\sim 200\ \mu\text{s}$) may relate to processes involved in the evolution of the jet outside the nozzle, they are unlikely to provide accurate information about the fluid properties most relevant to its ejection, unless there is an established theoretical basis for extending the frequency variation by at least an order of magnitude. Measurements at still higher frequencies will be of major interest for this purpose and are underway. In the present work we have relied on the 5 kHz PAV characterization to represent the fluids outside the nozzle—elsewhere[13] we shall discuss aspects of ligament elongation and collapse, and also the influence of elasticity on the jet ejection process.

While Dong et al.[4] studied drop formation in drop on demand printing for fluids having relatively low viscosity and relatively high surface tension compared with the viscoelastic fluids used in the present work, their analysis of ligament collapse and recoil is instructive. For three Newtonian fluids with viscosity of $\sim 1-5$ mPa s and surface tension between 33 and 65 mN/m, their results for ligament recoil velocity are consistent with a capillary speed defined here by $\sqrt{(2\sigma/\rho R)}$ for the fluid with surface tension σ, density ρ, and ligament radius R. In their work[4] they define capillary speed in terms of the nozzle radius, but the physical origin of the recoil involves the ligament radius R.

For our fluid series this predicted recoil velocity would be about 6 m/s. In the present work, the ratio of break-up time t_b to the ligament collapse timescale t_1 was about 4–5 for the viscoelastic fluids (see Fig. 6); as our main drop speed V_1 was chosen to be ~ 6 m/s for all series, the ligament recoil speed for the fluids studied is given by $L(t_b)/3t_1 \approx V_1^* t_b/3t_1 \approx 6 \times 4/3 \approx 8-10$ m/s, which is significantly greater than the predicted capillary recoil speed. This shows that viscoelastic ligaments can recoil at a higher speed than Newtonian fluids. However, the total time taken for the viscoelastic recoil can be comparable with or exceed that for purely Newtonian fluids because the viscoelastic ligaments tend to be longer before break-up occurs. If the viscoelastic content is increased further, the effects of elasticity on the attached ligament tip deceleration may be sufficient to prevent ligament break off from the nozzle plane and cause it to emerge but then retract back inside the nozzle. A roughly constant velocity viscoelastic ligament re-

coil behavior may thus be restricted to a rather low concentration regime.

Although the present work has utilized relatively dilute polymer solutions, for which the molecular chains do not overlap in static solutions, it shows strong evidence for elastic effects in jetting. At higher polymer concentrations, even more pronounced effects are seen, for example for cellulose esters in good solvents,[14] although in that investigation the relevant viscoelastic moduli were not independently measured. The results presented here represent the first quantitative link between high frequency rheology and jetting performance for fluids with nominally identical low shear rate viscosity, i.e., ink jet fluids which could not be discriminated on the basis of conventional rheological measurements.

CONCLUSIONS

For fluids that show viscoelastic behavior, properties measured by low-shear rate viscometers are insufficient to characterize certain rheological properties that are important in ink jet printing, which typically involve rather short timescales. Rheological data measured by PAV at 5 kHz for a series of model fluids containing polystyrene in diethyl phthalate correlated well with measurements of ligament length in drop-on-demand printing and successfully distinguished between fluids which had the same low shear-rate viscosity. Measurements at even higher frequencies may also be useful.

Plots of overall ligament length against jet tip position, for different concentrations and polymer molecular weights, can be used to optimize jetting conditions and to compare the jetting of different ink formulations. A phenomenological model has been introduced to help compare these different conditions and provide a basis for understanding the quantitative effects of viscosity and viscoelasticity, from which some but not all aspects of ink jetting and printing quality can be assessed.

The ratio of elastic to total modulus $G'/|G^*|$ at high frequency ($\sim$5 kHz) may be used to characterize a viscoelastic fluid; a linear correlation was found between this elasticity ratio and the time at which the ligament detached from the nozzle. High values of this elasticity ratio are associated with higher polymer molecular weight or higher concentration, giving fluids which either will not jet or cannot be printed due to the presence of extremely long ligaments.

ACKNOWLEDGMENTS

The authors thank N. Willenbacher, Karlsruhe University, Germany, for introducing one of the authors (T.R.T.) to the PAV technique and W. Pechhold, University of Ulm, Germany, for subsequent discussions. This research is supported by the UK EPSRC and industrial partners in the Next Generation Ink Jet Printing Consortium. One of the authors (T.R.T.) is now at Xaar plc, Cambridge.

REFERENCES

[1] I. M. Hutchings, G. D. Martin, and S. D. Hoath, "High speed imaging and analysis of jet and drop formation", J. Imaging Sci. Technol. **51**, 438 (2007).
[2] G. D. Martin, I. M. Hutchings, and S. D. Hoath, "Jet formation and late-stage ligament instability in drop-on-demand printing", *Proc. IS&T's NIP22* (IS&T, Springfield, VA, 2006) pp. 95–98.
[3] S. D. Hoath, G. D. Martin, J. R. Castrejón-Pita, and I. M. Hutchings, "Satellite formation in drop-on-demand printing of polymer solutions", *Proc. IS&T's NIP23* (IS&T, Springfield, VA, 2007) pp. 331–335.
[4] H. M. Dong, W. W. Carr, and J. F. Morris, "An experimental study of drop-on-demand drop formation", Phys. Fluids **18**, 072102 (2006).
[5] B. Brice Lopez, D. Vadillo, P. Pierron, and A. Soucemarianadin, "Transient Phenomena During Drop Formation In DOD Printing", *Proc. IS&T's NIP18* (IS&T, Springfield, VA, 2002) p. 170.
[6] C. Wagner, Y. Amarouchene, D. Bonn, and J. Eggers, "Drop detachment and satellite bead formation in viscoelastic fluids", Phys. Rev. Lett. **95**, 164504 (2005).
[7] T. R. Tuladhar and M. Mackley, "Filament stretching rheometry and break-up behavior of low viscosity polymer solutions and ink jet fluids", J. Non-Newt. Fluid Mech. **148**, 97–108 (2008).
[8] J. J. Crassous, R. Regisser, M. Ballauff, and N. Willenbacher, "Characterization of the viscoelastic behavior of complex fluids using the piezoelastic axial vibrator", J. Rheol. **49**, 851 (2005).
[9] G. H. McKinley and T. Sridhar, "Filament stretching rheometry of complex fluids", Annu. Rev. Fluid Mech. **34**, 375–415 (2002).
[10] J. de Jong, R. Jeurissen, H. Borel, M. van den Berg, H. Wijshoff, H. Reinten, M. Versluis, A. Prosperetti, and D. Lohse, "Entrapped air bubbles in piezo-driven ink jet printing: their effect on the droplet velocity", Phys. Fluids **18**, 121511 (2006).
[11] N. Reis, C. Ainsley, and B. Derby, "Ink jet delivery of particle suspensions by piezoelectric droplet ejectors", J. Appl. Phys. **97**, 094903 (2005).
[12] B.-J. de Gans, E. Kazancioglu, W. Meyer, and U. S. Schubert, "Ink jet printing polymers and polymer libraries using micropipettes", Macromol. Rapid Commun. **25**, 292 (2004).
[13] S. D. Hoath, I. M. Hutchings, G. D. Martin, O. Harlen, T. R. Tuladhar, M. R. Mackley, D. Vadillo, M. Knott, and T. C. B. McLeish, "Influence of polymer molecular weight on ink jet fluid jets", J. Polym. Sci. B: Polym. Phys. (unpublished).; S. D. Hoath, G. D. Martin, and I. M. Hutchings, "Methods and results from the Cambridge Inkjet Research Center", Invited talk at NSTI Nanotech 2009, Vol. 3, pp. 498–500, www.nsti.org
[14] D. Xu, V. Sanchez-Romaguera, S. Barbosa, W. Travis, J. de Wit, P. Swan, and S. G. Yeates, "Ink jet printing of polymer solutions and the role of chain entanglement", J. Mater. Chem. **17**, 4902–4907 (2007).